International Journal of Sediment Research 39 (2024) 552–559

Contents lists available at ScienceDirect

International Journal of Sediment Research

journal homepage: www.elsevier.com/locate/ijsrc

Original Research

Implications of bioturbation induced by *Procambarus clarkii* on seepage processes in channel levees

Michele Bendoni [a, b], Giuseppe Mazza [c], Nicola Savoia [d], Luca Solari [d, *], Elena Tricarico [e]

[a] LAMMA Consortium, Via Madonna del Piano 10, 50019, Sesto Fiorentino, Florence, Italy
[b] Institute of Marine Sciences - National Research Council of Italy (CNR-ISMAR), Forte Santa Teresa, 19032, Lerici, Italy
[c] CREA Research Centre for Plant Protection and Certification (CREA - DC), Via Lanciola 12/a, 50125, Cascine Del Riccio, Florence, Italy
[d] Department of Civil and Environmental Engineering, University of Florence, Via di Santa Marta 3, 50139, Florence, Italy
[e] Department of Biology, University of Florence, Via Madonna del Piano 10, 50019, Sesto Fiorentino, Florence, Italy

ARTICLE INFO

Article history:
Received 17 January 2023
Received in revised form
22 December 2023
Accepted 4 February 2024
Available online 8 February 2024

Keywords:
Burrowing activity
Channel banks and levees
Crayfish
Seepage flow
Internal erosion
Levee breach

ABSTRACT

River levees are subject to bioturbation by various animals which can actively excavate into earthen structures producing an internal erosion that, during the passage of a flood, can grow in time making the levee unstable. This phenomenon can lead to river levee breaching and, as a consequence, collapse, even for relatively minor flood events. A well-known animal burrower is represented by the North American crayfish *Procambarus clarkii* (*P. clarkii*), an invasive species in Europe, mainly introduced for commercial purposes, causing a decline in biodiversity and profound habitat changes. The physical damages caused by *P. clarkii* on levees and banks, such as in rice fields, irrigation ditches, and small channels, have not been fully studied and behavioral components underlying this impact are mostly occasional. To understand the impact of burrowing activity on the seepage process, a field survey was done in a drainage channel in Tuscany, Italy, to evaluate the density and geometry of the internal burrows that were excavated by the crayfish. Based on these observations and some previous laboratory experiments, three dimensional (3D) numerical simulations of the seepage processes were done inside burrowed levees. Numerical results allowed the increase in the hydraulic vulnerability of levees to the process of internal seepage to be disclosed. In particular, for a given river water level, the reduction of the time scale for the phreatic line to reach the levee field side appears to be a function of a quantity here defined as the burrow hydraulic gradient. This quantity is here defined as the ratio between the hydraulic head inside the burrow and the horizontal distance from its end to the field side of the levee. Moreover, a comparison between the 3D with the analogous more common two dimensional (2D) numerical simulations illustrated the schematization which is better suited for describing the seepage processes when animal burrows, not only by crayfish, are present.

1. Introduction

In recent years, alien species introductions have exponentially increased in Italy as well as in Europe, causing damage to ecosystems and human activities (Pagad et al., 2022; Seebens et al., 2017). In aquatic environments, the red swamp crayfish *Procambarus clarkii* (*P. clarkii*) is one of the most well-known invasive species (e.g., Souty-Grosset et al., 2016) and is indeed included in the List of Invasive Alien Species of Union concern linked to the European Union (EU) Regulation 1143/2014 on Invasive Alien Species. Its biological features, such as adaptability to different environments, plasticity of the biological cycle, feeding habit (omnivorous and generalist), resistance against diseases, and high reproductive rate, allow the species to successfully invade diversified habitats, being difficult to eradicate once established (Gherardi et al., 2011; Manfrin et al., 2019).

In addition to the impact on biodiversity (Savini et al., 2010), *P. clarkii* is responsible for the weakening of the small channel levees and the increase of water turbidity due to its digging activity. Indeed, burrows can be characterized by long and non-linear tunnels developing within the artificial or natural banks of riverine and lacustrine environments (Ceccato et al., 2022; Souty-Grosset et al.,

* Corresponding author.
E-mail address: luca.solari@unifi.it (L. Solari).

https://doi.org/10.1016/j.ijsrc.2024.02.001

2016) and remediation strategies are under investigation (Lemmers et al., 2022).

The effect of animals as active hydro-geomorphological agents is increasingly acknowledged in the literature (see for instance Rice, 2021; Sanders et al., 2021). In the case of earthen hydraulic structures, such as river levees, bioturbation can alter both the hydraulics and the stability of the structure because internal cavities weaken the structural integrity of embankments (Harvey et al., 2019) and can lead to their failure with catastrophic consequences. Orlandini et al. (2015) demonstrated the fundamental role of animal burrowing by the wildlife (such crested porcupine, red fox, and nutria) in the levee failure that occurred in 2014 in the Secchia River in Emilia-Romagna (North Italy) during a relatively minor flood event. Indeed, for channel levees and dams, the hydraulic alterations include shortening of seepage paths and steeper hydraulic gradients that can lead to an increase in the speed of internal soil erosion, and, thus, to a structural failure (Bayoumi & Meguid, 2011; Ceccato et al., 2022). Internal erosion, typically in the shape of piping, is triggered by the seepage process which promotes the enlargement of animal cavities through the formation of hydraulic fractures in the levee structure. These fractures favor the removal of soil particles enlarging the preferential path, and, thus, inducing positive feedbacks between removal rate and filtration flow until the scoured tunnel is large enough to eventually produce a bank instability and failure (Ceccato et al., 2022). Furthermore, the presence of burrows on the river bank, even if shorter than the width of the levee, reduces the lengths of seepage path and the associated hydraulic time scale for the rise of the phreatic line on the land side (Palladino et al., 2020). This mechanism can lead to a substantial increase in the vulnerability to seepage processes when the hydraulic time scale is somehow comparable to the time scale of the flood event (Michelazzo et al., 2018).

The evaluation of the impact of bioerosion on the hydraulics of levees requires: i) knowledge on the geometry of the internal cavities produced by the animal which can be typically obtained by using some *in situ* geophysical techniques (Borgatti et al., 2017; Chlaib et al., 2014; Masi et al., 2020) or, in some particular case, by doing laboratory experiments with the animal excavating into the soil structure (see for instance Haubrock et al. (2019) for the case of crayfish), ii) mathematical modeling of the seepage flow which can be achieved either using some analytical methods (Michelazzo et al., 2018; Palladino et al., 2020) or numerical simulations (Calamak et al., 2021). Numerical modeling is typically done considering a two dimensional (2D) geometrical configuration of the animal burrowing; however, this approximation is useful for the assessment of the vulnerability of levees to seepage flow in the case of long river reaches, while the burrows have a three dimensional (3D) structure. The effects of a more realistic 3D structure of the burrows on the seepage flow are still unexplored.

The current study focuses on the analysis of the effect of the burrowing activity of *P. clarkii* on the seepage processes occurring within banks and small levees that can be typically found in irrigation and urban channels. The work is based on a combined approach that includes both field monitoring of the burrows that were excavated by *Procambarus clarkii* in a cohesive drainage channel dissecting the Fucecchio marshes (Tuscany, Central Italy) and numerical modeling of the seepage flow considering the 3D geometry of the internal cavities. The main aims are to: i) identify the characteristic size and structure of burrows in the field, and ii) evaluate the hydraulic time scale of 3D seepage flow in small levees considering various burrowing configurations. The hydraulic time scale is here defined as the time for the phreatic line to emerge on the land side of the levee. The numerical simulations were also done in the case of idealized 2D configurations of the burrows to explore the differences between numerical approaches on the hydraulic time scale and disclose the conditions that allow application of a simpler and faster 2D approach.

2. Study area and field monitoring

The study area is represented by the Fucecchio Marshes which cover an area of about 1,800 ha, divided among the Provinces of Pistoia, Lucca, and Florence (Fig. 1). Today, it is the largest inland marsh in Central Italy, even if it once covered most of the southern Valdinievole. The area is densely populated by *P. clarkii* since the 2000 s as can be seen from the intense burrowing activity of the drainage channels (Fig. 2). A study area composed of straight muddy (silt and clay) channels with cohesive banks of about 45° inclination and a bed width of 2.6 m was considered. At the time of field surveys (July 2018), the channel was dry.

Field surveys were done in a 21 m long reach (Fig. 3). Casts of the found burrows were obtained by injecting polyurethane foam inside the dens; after its solidification, the soil was accurately removed, and the casts were taken to the hydraulics laboratory at the Department of Civil and Environmental Engineering of the University of Florence. For each cast, the following parameters were measured: intrinsic and cartesian lengths; diameters of three different cross sections (beginning, middle, end of the cast); and volume. In a few cases (see red circles in Fig. 3), 3D digital models of the casts were produced by photogrammetry (Agisoft PhotoScan), through the acquisition and processing of about 200 photographs of each cast.

3. Methodology

The finite element model Midas GTS NX (https://www.cspfea.net/portfolio_page/midas-gts-nx/) is applied to analyze the effect of the burrow dimensions, geometry, and characteristics on the seepage process. Midas GTS NX is a widely used software in geotechnical engineering and soil mechanics, and is also applied to simulate transient seepage flows in unsaturated media under various settings (e.g., Ceccato et al., 2021; Wang et al., 2020). The numerical modeling included two sets of different simulations: 3D with (t_{3D}) and without ($t_{3D,ind}$) burrows and 2D vs. 3D with burrows.

3.1. 3D numerical simulations with and without burrows

The first set of model runs was aimed to analyze the effect of the presence of burrows on the internal hydraulic time scale here identified with the failure time; i.e., the time for the saturation line to reach the land side of the levee. Based on previous laboratory experiments (Haubrock et al., 2019) and on the reported field monitoring, burrows were schematized as circular cylinders with a diameter of 5 cm with an entrance located near the levee bottom (Figs. 4 and 5). Different typologies of burrows having different lengths and widths were analyzed to identify the configurations corresponding to the largest differences compared to the undisturbed (undamaged) condition. For each model run, the water level on the river side of the levee was kept constant, and the simulation continued until the saturation line reached the other side of the levee. Such time, identified as the failure time, was determined for both the burrowed t_{3D} and undisturbed $t_{3D,ind}$ models. To compare various flow characteristics within the levee, in relation to the different burrowing configurations, a measure of the hydraulic gradient associated with each burrow is proposed and defined as $i = L_y/L_x$ with L_y being the hydraulic head in the burrow associated with the river water level, and L_x the minimum horizontal distance to the field side of the levee (Fig. 5c). Comparatively higher values of

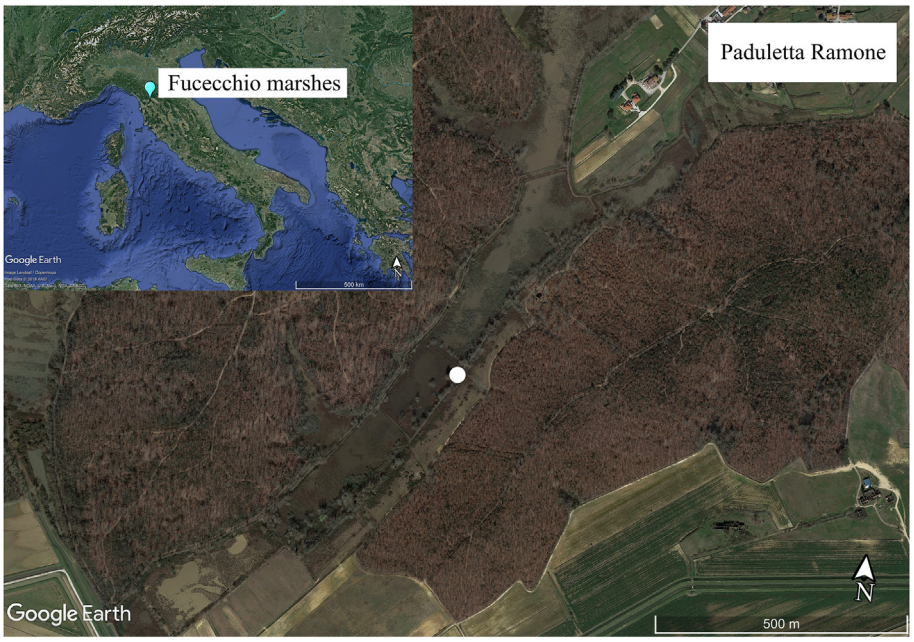

Fig. 1. View of the study area "Paduletta Ramone" located in the Fucecchio marshes. The white dot indicates the channel where the field survey was done.

Fig. 2. Picture of a channel bank affected by burrowing activity: (a) highlights of the burrows entrances (red circles); (b) *P. clarkii* in the burrow; and (c) burrows with a plug covering their entrance to maintain soil moisture.

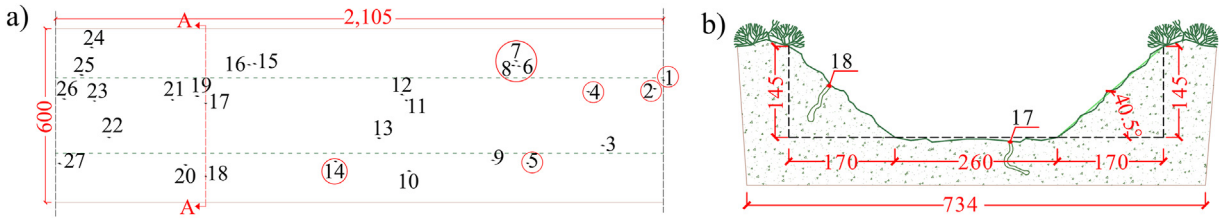

Fig. 3. (a) Plan view of burrows identified in the 21 m long reach; and (b) cross section *A–A* (dimensions are in mm).

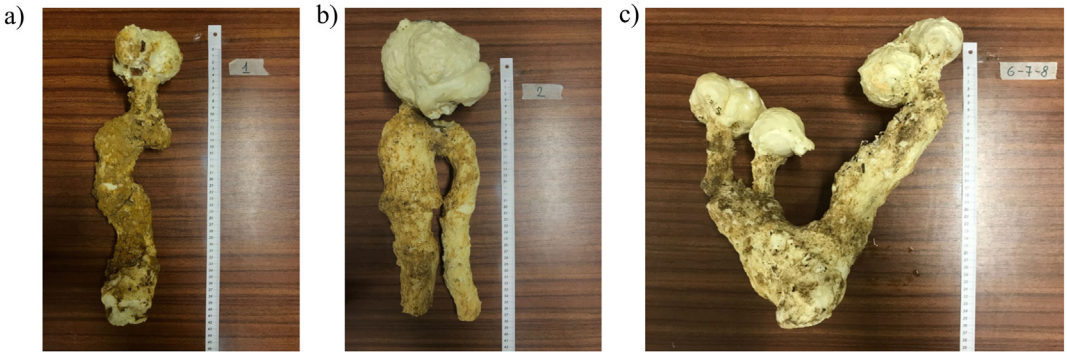

Fig. 4. Three typical burrow systems observed in the field: a) #1; b) #2; and c) #6-7-8. The expanded foam indicates the burrow entrances (dimensions are given in cm).

this parameter indicate either a burrow with a larger hydraulic head or a burrow closer to the levee land side.

3.2. 2D and 3D numerical simulations with burrows

The second set of numerical simulations was aimed at the estimation of potential differences between the 3D approach and the more commonly used 2D approach for evaluating seepage processes in levees even in the case of animal burrowing (Calamak et al., 2021; Palladino et al., 2020). The 2D approach simulated the seepage process on a vertical plane per unit width of the considered levee, whereas the 3D approach reproduced the whole length of the levee. First, it was verified that the two approaches converged to a unique solution in the case of a 3D model implementation with a 2D geometry (Fig. 5a). This aimed at excluding that alternative numerical implementations of 3D burrows differed from the corresponding 2D case due to model inaccuracies. Then, the focus shifted to the differences between 2D and fully 3D configurations, i.e., a circular hole starting from the upstream side of the levee (Fig. 5b). The boundary conditions for this set of experiments were the same applied to investigate the effect of burrows with respect to an undisturbed levee. Failure time was determined for both the 2D and 3D models, t_{2D} and t_{3D}, respectively.

The simulations were done on schematic levee models (Fig. 5c), having a comparable size to the experimental model utilized by Haubrock et al. (2019), and spatial scales similar to those found in the field (Figs. 2 and 4). The longitudinal dimension of the levee was set equal to 1 m (in this case a single burrow was considered). The soil was assumed to be linear, elastic, and isotropic, Young's modulus, E, was set to 5 MPa, Poisson's ratio, ν, was set to 0.4, and the hydraulic conductivity, k_h, was set to 10^{-8} m/s. A tetrahedral mesh with an average size of the order of 3.8 cm was utilized to discretize the spatial domain and the time step was set to 60 s. Different input parameters are surely affecting the results of numerical simulations specifically regarding the hydraulic time scale; however, it is expected that the main conclusions that are derived from the current study still hold true.

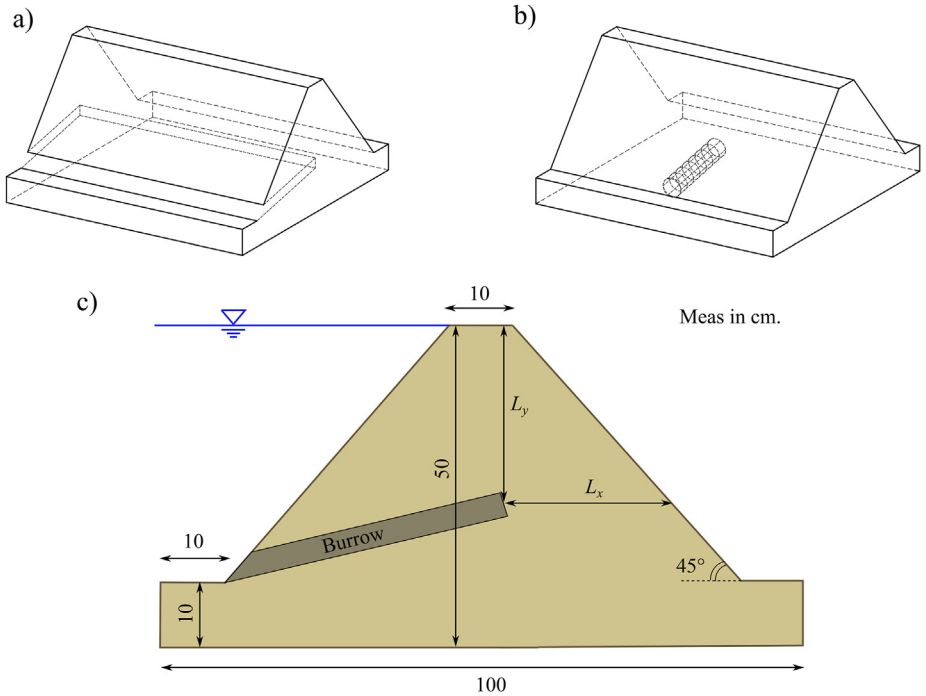

Fig. 5. Sketch of the levees considered to simulate the equivalence with the 2D a), and the corresponding 3D case b). Sketch of the levee considered for the simulations with dimensions and the identification of the quantities L_x and L_y used for calculating the burrow hydraulic gradient c).

Table 1
Geometric characteristics of the foam casts retrieved from the field burrows. D_{in} = diameter of the burrow at the entrance; D_{middle} = diameter of the burrow in the middle length; D_{out} = diameter of the burrow at the end.

Sample		Intrinsic length (cm)	Cartesian length (cm)	D_{in} (cm)	D_{middle} (cm)	D_{out} (cm)	Volume (cm^3)
1		41	30.5	4	6.5	7	500
2	left branch	35	29.5	4.5	8.5	4.5	1,000
	right branch	34.5	33.5	4.5	5.5	3.5	
3		31	29.5	3	7.5	4	800
4		41	33	5.5	6.5	4.5	600
5		56	46	5	5.5	5	800
6		38	28	5	9	7.5	1,800
7		19	7	4.5	3.5	3	
8		24	12	3.5	3.5	4	
9		42	28.5	3.5	5	7.5	400
10		30	27	13	8	10	500
11		23	17	4	5	9.5	300
12	left branch	18	19.5	4.5	4.5	5	200
	right branch	21.5	16	4.5	3.5	8	
13		24	16.5	3	6	10.5	200
14		16	15.5	8	5	3.5	300
15		35	31	3.5	3	4.5	400
16		25	21.5	6	8	7	500
17		29	26	4	4.5	3.5	300
18		19	19	3.5	3	4.5	300
19		38	28.5	4.5	8.5	6.5	700
20		30	24	5	7	5.5	400
21		24	22.5	5	3.5	4	300
22		41	33.5	4	4	6	400
23		17	16.5	3	4	5	200
24		27	24.5	5.5	5	6	500
25	left branch	26	11.5	5	3.5	3	400
	right branch	19	17	5	3.5	2	
26		18	16	4.5	9	4	300
27		18	18.5	3.5	3	5.5	200

4. Results and discussion

4.1. 3D numerical simulations with and without burrows

In the field section, 27 burrows were observed (Table 1), thus, the average linear density was 1.3 burrow/m. The mean geometric characteristics of the 27 casts replicating the field burrows were: volume 506 ± 342 mL; intrinsic length 29.5 ± 9.7 cm; cartesian length 24 ± 8 cm; and opening diameter at the entrance 4.6 ± 1.8 cm (where ± indicates one standard deviation bounds on the mean). These burrows appeared to be smaller, in terms of both length and volume, than the structures observed in the laboratory experiments (Haubrock et al., 2019) while the diameters were very much similar with a mean of 4.8 ± 0.9 cm. The reason for this difference (shorter tunnels in the field than in the laboratory) might be associated to different field conditions such as due to rapid water retreat in the channel, and, therefore, shorter time for animals to excavate the burrows. The main observed shapes were cylindrical; multiple openings ending in one final chamber; single opening with two tunnels (Fig. 4). These shapes are overall consistent with the structures that the animals excavated in the laboratory as reported in the literature (Haubrock et al., 2019).

The configuration of the saturation surface for a generic numerical experiment, after 2,400 s from the beginning of the simulation, is shown in Fig. 6(a); at this time, it appears that the burrow greatly shifts the phreatic surface towards the land side, however, its influence is limited to a region neighboring the burrow itself while in the remaining portion of the levee seepage flow does not seem to be altered. Figure 6(b) illustrates the corresponding values of the pore pressure along a vertical plane that intersects the middle of the levee. The impact of the burrows on the failure time has previously been assessed by other authors (see for example, Palladino et al., 2020). Basically, the reduction of the time necessary to reach the critical condition is the main evidence.

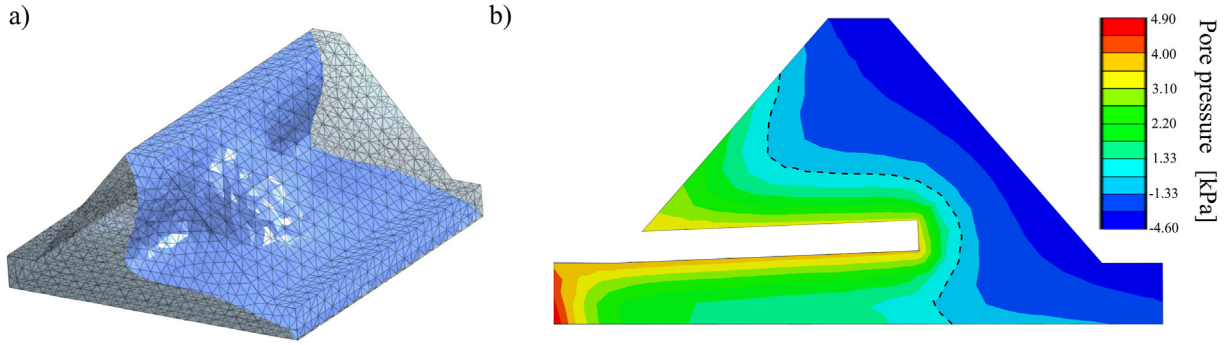

Fig. 6. a) View of the saturation surface after 2400 s from the beginning of the simulation. b) Section of the levee showing the pore water pressure after 2400 s from the beginning of the simulation (water level on the river side is imposed at the top of the levee; saturation line, black dashed line, is defined by pore pressure equal to zero).

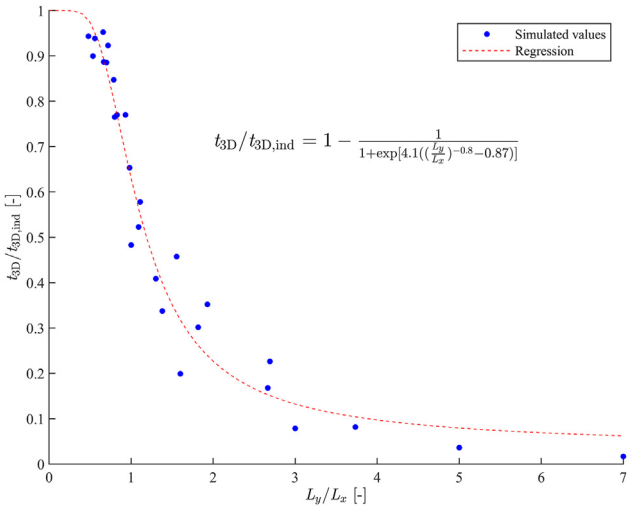

Fig. 7. Trend of the relative failure time (ratio between the failure time of burrowed levee to the failure time for the undisturbed levee) with respect to the burrow hydraulic gradient ($i = L_y/L_x$). Blue circles represent simulated values while red-dashed line is the regression curve.

Figure 7 shows the ratio between the failure time, $t_{3D,}$ for a burrowed levee with respect to the undisturbed time, $t_{3D,ind}$, as a function of the burrow hydraulic gradient L_y/L_x together with the nonlinear fitting of the data using the equation reported on the plot, with a coefficient of determination (R^2) = 0.96. The analysis shows that the failure time can be expressed as a monotonic function rapidly decreasing with the burrow hydraulic gradient. In particular, when L_y/L_x is greater than 1 (burrow either having a relative great hydraulic head L_y and/or relative shorter distance to the land side L_x), t_{3D} appears to be about 60% of the undisturbed time $t_{3d,ind}$.

For the sake of simplicity, the hydraulic conductivity of the levee is kept constant and the simulations are not repeat changing this parameter. Hydraulic conductivity can indeed be different, based on soil typology, or can be even perturbed in the surrounding of the burrow as a consequence of the digging activity. When the hydraulic conductivity changes for the whole levee, it is suggested that the main results would be qualitatively confirmed, since a general increase or decrease of the seepage process is expected over the whole levee. Perturbed values of hydraulic conductivity in the surrounding of the burrow may lead to substantial changes in the pore pressure distribution when compared to case of spatially uniform hydraulic conductivity. Nevertheless, in both cases, a specific set of experiments is required to systematically test the aforementioned changes.

4.2. 2D and 3D numerical simulations with burrows

Differences between the failure time calculated using a 2D schematization and that with the 3D approach varying with the burrow hydraulic gradient are shown in Fig. 8. As expected, t_{3D}/t_{2D} is always greater than 1 with a maximum of about (1.8−1.9) for L_y/L_x between 2 and 3 corresponding to burrow configurations ending close to the land side (configurations B and C). The behavior of the 2D and 3D approaches appears to be similar for small and very large hydraulic gradients, with $L_y/L_x \approx 1$ and $L_y/L_x \approx 7$ for configurations D and A, respectively. This result suggests that a 2D approximation of burrow geometry might lead to much shorter failure times. This indicates that 2D simulations in the case of animal burrowing can lead to substantially cautious, if not unrealistic, evaluations regarding the vulnerability of levees to seepage for a given persistence of the flood levels (Michelazzo et al., 2018).

The comparison between 2D and 3D simulations is further extended to evaluate the effect of multiple adjacent burrows on the hydraulic seepage process, as observed in the field (Fig. 3). The aim is to identify some thresholds in the linear spacing density of the burrows above which the results can be approximated using a 2D approach, while for a smaller density (i.e., burrows at a greater relative distance, b_{dist}) a more realistic 3D approach needs to be applied. In the simulations, the configuration "B" (Fig. 8) is reproduced according the following spacings, b_{dist}: 0.1, 0.25, 0.45, 0.6, 0.8, 1.0, and 1.2 m for a fixed burrow diameter b_{diam} = 5 cm. To limit the effect of the lateral boundaries of the levee, numerical runs with multiple parallel burrows were done by extending the levees by 1.5 m on each side from the most external burrow. Figure 9 shows the numerical results showing that t_{3D}/t_{2D} ranges from about 1

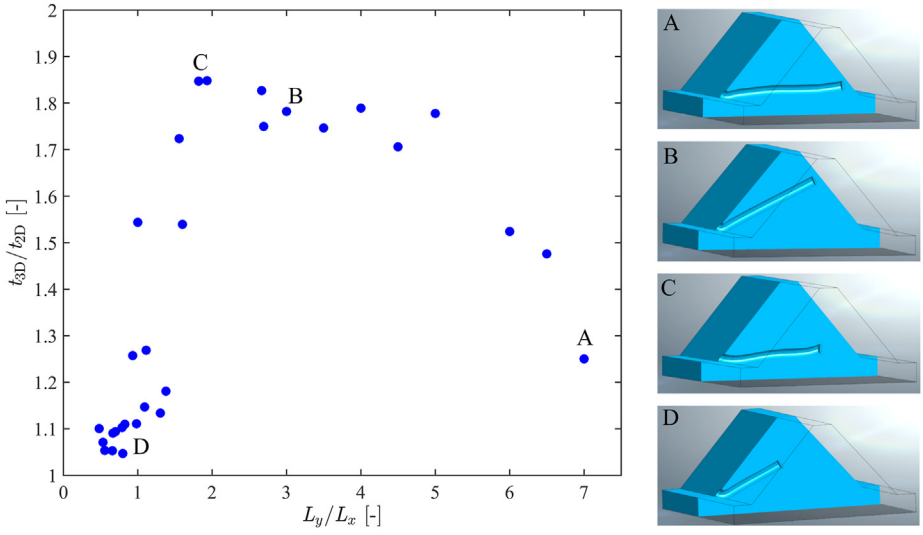

Fig. 8. Ratio of the failure time for a 3D burrowed levee to the failure time of the 2D case, as a function of the burrow hydraulic gradient, L_y/L_x, for different configurations of the burrow (right sketches, from A to D).

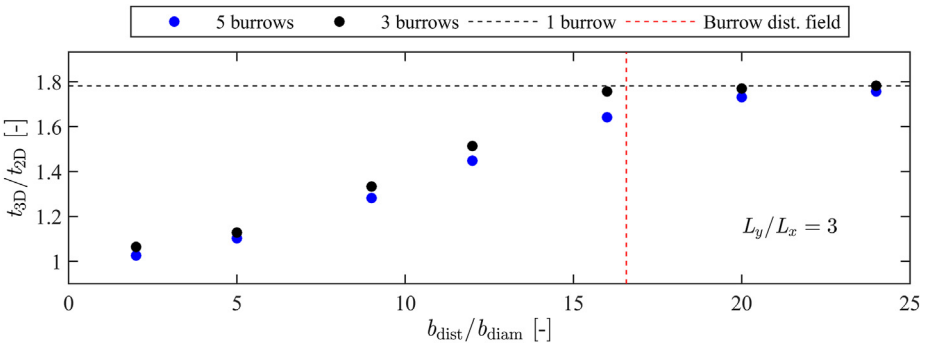

Fig. 9. Ratio of the failure time for a series of burrows (5 burrows, blue dots; 3 burrows, black dots) at variable distance, to the failure time of the 2D burrowed levee configuration, as a function of the ratio between burrow distance and burrow averaged diameter (≈5 cm). Black dashed line represents the ratio t_{3D}/t_{2D} for a single burrow. Red dashed line refers to the average burrow spacing characteristics observed in the field. The simulated burrowed levee corresponds to configuration B (Fig. 8).

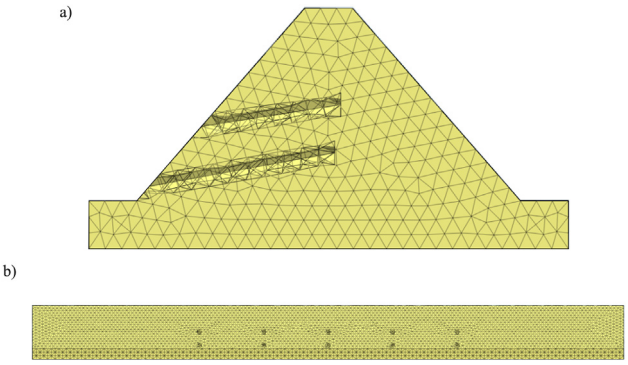

Fig. 10. Simulated geometry of multiple burrows according to two rows; example with 5 burrows in each row and $b_{dist}/b_{diam} = 12$. Lateral view a) and frontal view b).

when spacing is very low (b_{dist}/b_{diam} of about 1) to the maximum of about 1.8 in the case of large spacing (b_{dist}/b_{diam} of about 20). In the latter case, each burrow is not interfering with the other neighboring burrows, thus, the burrows act as being hydraulically isolated. Moreover, field observations show an average b_{dist}/b_{diam} of about 16, thus, neighboring burrows hydraulically do not act as being either isolated ("large" b_{dist}/b_{diam}) or fully interfering ("small" b_{dist}/b_{diam}). This result is obtained considering all the burrows having the same configuration B, however, field observations illustrate a range of different geometries, therefore, future research might address these aspects.

Since the burrows observed in the field display a rather complex network, the previous results (Fig. 9) are expanded by considering an additional row of burrows having the entrance in the middle of the height of the levee (Figs. 10a and 10b); the investigated configuration is characterized by $L_y/L_x = 1$ which, in the case of a single burrow (Fig. 8), is characterized by t_{3D}/t_{2D} of about 1.1. Results (Fig. 11) show that the effect of an additional row of burrows further increases the differences between t_{3D} and t_{2D}; in particular, when the burrows are at sufficiently large distance, b_{dist}/b_{diam} >10, t_{3D}/t_{2D} approaches 2.6, thus, indicating a large difference between 3D and 2D simulations.

5. Conclusions

In this work, the burrowing activity of the invasive crayfish *Procambarus clarkii* in cohesive banks and levees of lowland channels and the implications on seepage flow is explored. The research methodology included a field survey of the excavated burrows in a channel in the Fucecchio marshes in Tuscany (Central Italy) and 3D numerical modeling of the seepage flow inside the river levee considering various geometric configurations of the burrows. The effect of the burrow on the seepage flow was assessed through the evaluation of the hydraulic time scale defined as the time required for the saturation line to reach the land side of the levee; this is the necessary condition defining the failure of the levee. According to the current field observations and some previous laboratory experiments done by the authors, different burrow configurations were numerically reproduced. The results show that the hydraulic time scale or failure time can be expressed as a decreasing function of the burrow hydraulic gradient here defined as the ratio between the hydraulic head imposed in the burrow and its minimum distance

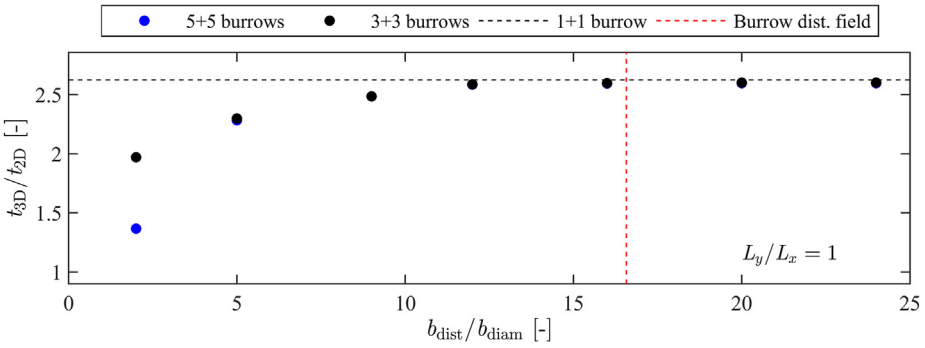

Fig. 11. Effects of two rows of burrows on the failure time t_{3D} (5 + 5 burrows, blue dots; 3 + 3 burrows, black dots) at variable distance, to the failure time t_{2D} of the 2D burrowed levee configuration, as a function of the ratio between burrow distance and burrow average diameter (≈5 cm). Black dashed line represents the ratio t_{3D}/t_{2D} for a single burrow in each row. Red dashed line refers to the average burrow spacing characteristics observed in the field.

to the land side of the levee. Numerical analysis was further extended to disclose the differences between the proposed 3D approach and the more common 2D schematization applied in the case of river levees.

Based on the foregoing analysis, the following main conclusions can be derived.

- 27 burrows were observed over a channel reach 21 m long; the burrows have an intrinsic length of 29.5 ± 9.7 cm; cartesian length 24 ± 8 cm, and opening diameter at the entrance 4.6 ± 1.8 cm;
- 3D numerical modeling revealed that the presence of burrows drastically reduces its relative failure time when the burrow hydraulic gradient is already about 1 (i.e., burrows either having a greater internal hydraulic head or closer to the land side of the levee) considering a relatively high water level on the river side as in river flood conditions;
- the comparison of the proposed 3D schematization with the analogous 2D numerical simulations demonstrates that failure time is always greater in the 3D case, and approaches the 2D case when the distance between the burrows is in order of few times the burrow diameter. This is even more apparent in the case of burrows located in multiple rows.

Future research might include the extension of the 3D numerical simulations to further geometrical configurations of burrows including those by other animals, such as beaver, recently reintroduced in Italy (Pucci et al., 2021), coypu, and crested porcupine. Also, research regarding the dynamics of seepage flow in the case of varying river water levels as during a flood event, and by varying the hydraulic conductivity of the levee to account for the effect of the digging activity in perturbing the soil characteristics in the surroundings of the burrow, and for different soil typologies should be considered.

Declaration of competing interest

The authors declare that they have no known competing financial interests or personal relationships that could have appeared to influence the work reported in this paper.

Acknowledgements

This work was supported by the National Recovery and Resilience Plan (NRRP), Mission 4 Component 2 Investment 1.4 – Call for tender No. 3138 of December 16, 2021, rectified by Decree n.3175 of December 18, 2021 of the Italian Ministry of University and Research funded by the European Union – NextGenerationEU. Cosimo Tellini is gratefully acknowledged for his important support with the numerical simulations.

References

Bayoumi, A., & Meguid, M. A. (2011). Wildlife and safety of earthen structures: A review. *Journal of Failure Analysis and Prevention, 11*, 295–319.

Borgatti, L., Forte, E., Mocnik, A., Zambrini, R., Cervia, F., Martinucci, D., … Zamariolo, A. (2017). Detection and characterization of animal burrows within river embankments by means of coupled remote sensing and geophysical techniques: Lessons from River Panaro (northern Italy). *Engineering Geology, 226*, 277–289.

Calamak, M., Larocque, L. A., & Chaudhry, M. H. (2021). Numerical modelling of seepage through earthen dams with animal burrows: A case study. *Journal of Hydraulic Research, 59*(3), 488–499.

Ceccato, F., Simonini, P., & Zarattini, F. (2021). Case Study: Monitoring and modelling tidal-induced pore pressure oscillations in the soil of St. Mark's Square in Venice. *Journal of Geotechnical and Geoenvironmental Engineering, 147*(5), 1–14.

Ceccato, F., Malvestio, S., & Simonini, P. (2022). Effect of animal burrows on the vulnerability of levees to concentrated erosion. *Water, 14*, 2777.

Chlaib, H. K., Mahdi, H., Al-Shukri, H., Su, M., Catakli, A., & Abd, N. (2014). Using ground penetrating radar in levee assessment to detect small scale animal burrows. *Journal of Applied Geophysics, 103*, 121–131.

Gherardi, F., Aquiloni, L., Diéguez-Uribeondo, J., & Tricarico, E. (2011). Managing invasive crayfish: Is there any hope? *Aquatic Sciences, 73*, 185–200.

Harvey, G. L., Henshaw, A. J., Brasington, J., & England, J. (2019). Burrowing invasive species: An unquantified erosion risk at the aquatic-terrestrial interface. *Reviews of Geophysics, 57*, 1018–1036.

Haubrock, P. J., Inghilesi, A. F., Mazza, G., Bendoni, M., Solari, L., & Tricarico, E. (2019). Burrowing activity of *Procambarus clarkii* on levees: Analysing behaviour and burrow structure. *Wetlands Ecology and Management, 27*, 497–511.

Lemmers, P., van der Kroon, R., van Kleef, H. H., Verhees, J. J. F., Gvan der Velde, G., & Leuven, R. S. E. W. (2022). Limiting burrowing activity and overland dispersal of the invasive alien red swamp crayfish *Procambarus clarkii* by sophisticated design of watercourses. *Ecological Engineering, 185*, 106787.

Manfrin, C., Souty-Grosset, C., Anastácio, P. M., Reynolds, J., & Giulianini, P. G. (2019). Detection and control of invasive freshwater crayfish: From traditional to innovative methods. *Diversity, 11*(1), 5.

Masi, M., Ferdos, F., Losito, G., & Solari, L. (2020). Monitoring of internal erosion processes by time-lapse electrical resistivity tomography. *Journal of Hydrology, 589*, 125340.

Michelazzo, G., Paris, E., & Solari, L. (2018). On the vulnerability of river levees induced by seepage. *Journal of Flood Risk Management, 11*, 677–686.

Orlandini, S., Moretti, G., & Albertson, J. D. (2015). Evidence of an emerging levee failure mechanism causing disastrous floods in Italy. *Water Resources Research, 51*, 7995–8011.

Pagad, S., Bisset, S., Genovesi, P., Groom, Q., Hirsch, T., Jetz, W., … McGeoch, M. (2022). Country compendium of the global register of introduced and invasive species. *Scientific Data, 9*, 39.

Palladino, M. R., Barbetta, S., Camici, S., Claps, P., & Moramarco, T. (2020). Impact of animal burrows on earthen levee body vulnerability to seepage. *Journal of Flood Risk Management, 13*.

Pucci, C., Senserini, D., Mazza, G., & Mori, E. (2021). Reappearance of the Eurasian beaver *Castor fiber* L. in Tuscany (Central Italy): The success of unauthorised releases? *Hystrix, 32*, 182–185.

Rice, S. P. (2021). *Why so skeptical? The role of animals in fluvial geomorphology* (p. e1549). Water: Wiley Interdisciplinary Reviews.

Sanders, H., Rice, S. P., & Wood, P. J. (2021). Signal crayfish burrowing, bank retreat and sediment supply to rivers: A biophysical sediment budget. *Earth Surface Processes and Landforms, 46*, 837–852.

Savini, D., Occhipinti-Ambrogi, A., Marchini, A., Tricarico, E., Gherardi, F., Olenin, S., & Gollasch, S. (2010). The top 27 animal alien species introduced into Europe for aquaculture and related activities. *Journal of Applied Ichthyology, 26*(s2), 1–7.

Seebens, H., Blackburn, T. M., Dyer, E. E., Genovesi, P., Hulme, P. E., Jeschke, J. M., … Essl, F. (2017). No saturation in the accumulation of alien species worldwide. *Nature Communications, 8*(1), 14435.

Souty-Grosset, C., Anastácio, P., Aquiloni, L., Banha, F., Choquer, J., Chucoll, C., & Tricarico, E. (2016). Impacts of the red swamp crayfish Procambarus clarkii on European aquatic ecosystems and human well-being. *Limnologica, 58*, 78–93.

Wang, F., Ren, Q., Chen, B., Zou, P., Peng, Z., Hu, W., & Ma, Z. (2020). Numerical investigation on safe mining of residual pillar in goaf: A case study of panlong lead–zinc mine. *Geotechnical & Geological Engineering, 38*, 4269–4287.